Received: 23 May 2023 | Accepted: 21 August 2023

DOI: 10.1002/maco.202313931

SHORT COMMUNICATION

Materials and Corrosion

Investigating electrochemical charging conditions equivalent to hydrogen gas exposure of X65 pipeline steel

Erik Koren[1] | **Catalina M. H. Hagen**[2] | **Dong Wang**[1] | **Xu Lu**[1] | **Roy Johnsen**[1]

[1]Department of Mechanical and Industrial Engineering, NTNU, Trondheim, Norway

[2]SINTEF, Trondheim, Norway

Correspondence
Erik Koren and Xu Lu, Department of Mechanical and Industrial Engineering, NTNU, 7491 Trondheim, Norway.
Email: erik.a.koren@ntnu.no and xu.lu@ntnu.no

Funding information
Research Council of Norway, Grant/Award Number: 294739

Abstract

In this study, we systematically investigate electrochemical hydrogen charging conditions equivalent to hydrogen gas pressures relevant for hydrogen transportation in X65 pipeline steel. By performing hydrogen gas permeation, a relationship for Sieverts' law was established, which was used in combination with electrochemical hydrogen permeation to determine the equivalent hydrogen pressure. The results revealed that cathodic protection simulated condition at –1050 $mV_{Ag/AgCl}$ was equivalent to a hydrogen pressure of 12.3 bar. The addition of thiourea, a hydrogen recombination poison, and changing the applied potential in the cathodic direction increased the equivalent hydrogen pressure. In this way, an electrochemical charging condition equivalent to a potential hydrogen gas pressure for hydrogen transportation (200 bar) was determined.

KEYWORDS

electrochemical charging, equivalent fugacity, H_2 gas charging, hydrogen embrittlement, hydrogen permeation, pipeline steel

1 | INTRODUCTION

With hydrogen emerging as a clean energy carrier,[1] the transportation and storage of pressurized hydrogen gas have gained recent interest,[2–6] for example, repurposing existing natural gas pipelines for hydrogen gas transportation.[7] Pipelines should withstand pressures in the range 150–200 bar, due to the low energy density of hydrogen gas.[8] Hydrogen can degrade a material's mechanical properties, a phenomenon known as hydrogen embrittlement (HE).[9] Because of safety concerns using pressurized hydrogen gas, electrochemical charging is sometimes used as a substitute for hydrogen gas exposure during investigations of HE susceptibility of a material.[10,11] The severity of HE effects is highly dependent on the hydrogen charging condition.[2,12] Relating electrochemical and gaseous charging, would enhance the comparability of HE investigations performed under different charging conditions. The equivalence between electrochemical and gaseous charging has previously been investigated by hydrogen permeation,[13–16] thermal desorption analysis,[17–19] and by measuring the hydrogen pressure developed in a hollow sensor during charging.[20] While these studies investigated the pressure equivalency from common electrochemical charging conditions, a systematic approach to determine electrochemical charging conditions equivalent to pressures relevant for hydrogen gas transportation is lacking.

Chemical additives can enhance hydrogen absorption during electrochemical charging.[21,22] Several mechanisms explaining the increased hydrogen absorption have been proposed, which have been discussed in detail in Protopopoff and Marcus.[23] One prominent hypothesis is that the enhanced hydrogen absorption is caused by a chemisorbed element or species obstructing the recombination of adsorbed atomic hydrogen, hence, these additives are commonly referred to as hydrogen recombination poisons.[24] Increasing the cathodic current density or cathodic potential are other measures to enhance hydrogen uptake,[17,25] however, high cathodic current densities can cause unsteady surface conditions due to extensive bubble formation, changes in the local pH, or detachment of second phase particles.[26,27] Akiyama and Li investigated the application of hydrogen recombination poison and different cathodic current densities to optimize electrochemical charging,[22] however, its equivalence to gaseous hydrogen charging was not determined.

Herein, the objective is to optimize the electrochemical charging conditions to obtain a desired and predetermined equivalent hydrogen pressure, which simulates a potential hydrogen pressure level (200 bar) in a pipeline system aimed for hydrogen transportation.

2 | MATERIAL AND METHODS

2.1 | Material and sample preparation

The steel used in this study was API 5L X65 grade, from a quenched and tempered, seamless pipe. The wall thickness was 15.4 mm. It consisted of homogeneously distributed grains of ferrite and bainite. The phase volumes of ferrite and bainite were 89% and 11%, respectively. The average grain size was 7 μm. The chemical composition is given in Table 1. The samples were machined from a position close to the inner side of the pipe wall, parallel to the longitudinal direction. Plates with dimensions of 50 × 150 × 1.9 mm (width × length × thickness) were used for hydrogen gas charging. Disks with dimensions of 30 mm diameter and 1.1 mm thickness were used for electrochemical charging. The exposed areas during gaseous and electrochemical charging were 16 and 3.7 cm^2, respectively. Both sides of all samples were prepared with SiC grinding papers to a final grade of #P1000. A Pd coating was electrodeposited on the detection side of all samples, following the method described by Husby et al.[28] based on the work of Bruzzoni et al.[29] and Castaño Rivera et al.[30] Samples used for gas charging were also coated with Pd on the charging side. Pd facilitates hydrogen oxidation on the detection side,[31] while on the charging side, Pd is applied to overcome the surface impedance which can be caused by an oxide layer during gaseous hydrogen charging.[3,13,16]

TABLE 1 The chemical composition of the API 5L X65 studied steel.

Element	C	Si	Mn	P	S	Cu	Cr
wt%	0.07	0.22	1.19	0.011	0.003	0.14	0.15
Element	**Ni**	**Mo**	**V**	**Nb**	**Ti**	**N**	**Fe**
wt%	0.15	0.12	0.02	0.019	0.001	0.01	Bal.

2.2 | Hydrogen permeation tests

The hydrogen permeation experiments follow the principles first described by Devanathan and Stachurski.[32] A detailed description of the gas permeation set-up and electrochemical permeation set-up was described in a previous paper.[16] In the detection chamber, for both gas and electrochemical permeation, a 0.1 M NaOH solution (pH = 12.6) and an applied potential of +315 mV_{SCE} was used to ensure hydrogen oxidation. For gaseous hydrogen charging, the applied hydrogen gas pressures were 10, 50, and 100 bar. In the charging chamber, a 3.5 wt% NaCl solution (pH = 6.6) with an applied potential of −1050 $mV_{Ag/AgCl}$ was used to simulate cathodic protection (CP) conditions. To enhance the uptake of hydrogen, thiourea (CH_4N_2S) with various concentrations (0.5–3 g L^{-1}) was added and the cathodic potential was changed in steps of 75 mV in the cathodic direction. Two charging and discharging cycles were performed for all charging conditions. All tests were performed at room temperature (21 ± 1°C).

To determine the effective hydrogen diffusion coefficient, D_{eff}, partial permeation transients were conducted in a 3.5 wt% NaCl solution with a 2 g L^{-1} thiourea addition. Performing partial permeation transients can reduce surface and trapping effects, such that the permeation transients can be fitted to solutions of Fick's second law.[33] Initially, a charging potential of −1050 $mV_{Ag/AgCl}$ was applied until a steady permeation current density was achieved. Subsequently, the applied charging potential was changed every 5500 s in the following order: −1200, −1350, −1200, and −1050 $mV_{Ag/AgCl}$, such that two build-up transients and two decay transients were obtained.

2.3 | Analysis

The subsurface hydrogen concentration in lattice and reversible trap sites, C_{0R}, is proportional to the steady-state permeation current density, i_p^{∞}.[34] C_{0R} was calculated

using Equation (1), where L denotes the thickness of the sample and F denotes the Faraday constant (96,485 A s mol^{-1}).

$$C_{0R} = \frac{i_p^{\infty} L}{F D_{eff}}, \quad (1)$$

D_{eff} was determined by fitting the partial permeation transients to analytical solutions of Fick's second law to the build-up transient, Equation (2), and the decay transient, Equation (3).[33] i_p denotes the permeation current density, i_p^0 denotes the permeation current density at the time of changing the applied potential, t denotes the time after changing the applied potential, and D denotes the hydrogen diffusion coefficient.

$$\frac{i_p - i_p^0}{i_p^{\infty} - i_p^0} = \frac{2L}{\sqrt{\pi D t}} \sum_{n=0}^{\infty} \exp\left(-\frac{(2n+1)^2 L^2}{4Dt}\right), \quad (2)$$

$$\frac{i_p - i_p^{\infty}}{i_p^0 - i_p^{\infty}} = 1 - \frac{2L}{\sqrt{\pi D t}} \sum_{n=0}^{\infty} \exp\left(-\frac{(2n+1)^2 L^2}{4Dt}\right). \quad (3)$$

According to Sieverts' law, the amount of hydrogen dissolved in steel is proportional to the square root of the hydrogen fugacity, f_{H_2}, where S denotes Sieverts' constant.[35] At steady state, the lattice hydrogen concentration will scale as the reversibly trapped hydrogen concentration,[36] hence, Sieverts' law can be expressed as shown in Equation (4). f_{H_2} is related to the hydrogen pressure, p_{H_2}, through the Abel–Noble equation of state, Equation (5), where b denotes a constant (1.584×10^{-5} m^3 mol^{-1}), T denotes the temperature in K, and R denotes the gas constant (8.314 J K^{-1} mol^{-1}).[37] The method to determine the equivalent hydrogen fugacity, $f_{H_2}^{eq}$, is described in detail in a previous paper[16] and is based on work reported by Atrens and colleagues.[14,15,17] It is considered that charging conditions that produce the same C_{0R} in a steel are equivalent. In such matter, $f_{H_2}^{eq}$ was calculated by inserting C_{0R} determined from electrochemical charging into Equation (4) and solved for f_{H_2}. Then Equation (5) was solved iteratively using the Newton–Raphson method to determine the equivalent hydrogen pressure, $p_{H_2}^{eq}$, from $f_{H_2}^{eq}$.

$$C_{0R} = S \times \sqrt{f_{H_2}}, \quad (4)$$

$$f_{H_2} = p_{H_2} \exp\left(\frac{p_{H_2} b}{RT}\right). \quad (5)$$

3 | RESULTS AND DISCUSSION

The normalized partial permeation transients of the build-up and decay are presented in Figure 1a and 1b, respectively. The predicted solution of Fick's second law for lattice hydrogen diffusivity ($D_L = 7.27 \times 10^{-5}$ cm^2 s^{-1})[38] is included in the figures, as well as the average of the best fits to Equations (2) and (3). In alloys such as X65 pipeline steels, a significant trap occupancy can cause the normalized permeation transient to be steeper than predicted by Fick's second law.[39] The consequence can be a false interpretation of D_{eff}, which would appear to be changing with time.[39] By using the method of partial permeation transients, the effect of changing trap occupancy on the transient is reduced,[33] and the partial permeation transients can be fitted to the analytical solutions of

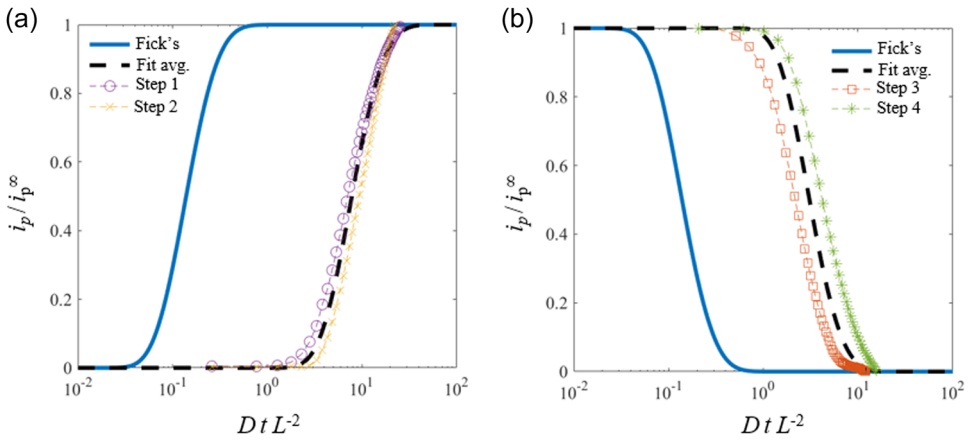

FIGURE 1 Normalized partial permeation transients obtained in a 3.5 wt% NaCl solution with a 2 g L^{-1} thiourea addition, including the prediction by Fick's second law for lattice diffusion and the average of the best fits. (a) Step 1: −1050 to −1200 $mV_{Ag/AgCl}$, Step 2: −1200 to −1350 $mV_{Ag/AgCl}$. (b) Step 3: −1350 to −1200 $mV_{Ag/AgCl}$, Step 4: −1200 to −1050 $mV_{Ag/AgCl}$. [Color figure can be viewed at wileyonlinelibrary.com]

Fick's second law. The average determined D_{eff} from the partial permeation transients is 2.3×10^{-6} cm^2 s^{-1}, which was used for the determination of C_{0R}.

Figure 2a shows two hydrogen permeation transients performed at 10, 50, and 100 bar. i_p^{∞} increases with increasing applied p_{H_2}, manifesting that the hydrogen flux through the samples increases with increasing p_{H_2}. C_{0R} determined from gas charging at 10, 50, and 100 bar is 0.031, 0.066, and 0.095 wppm, respectively. Figure 2b shows the hydrogen permeation transients obtained in CP-simulated conditions. The corresponding C_{0R} obtained is 0.032 wppm. As shown in Figure 2c, C_{0R} obtained from gas charging is proportional to $f_{H_2}^{1/2}$, which is consistent with Sieverts' law (Equation 4). The calculated S is 0.0095 wppm bar$^{-1/2}$, which is slightly lower than determined in a previous study for a hot rolled and welded X65 pipeline steel.[16] S is almost three times less than reported for a 3.5 NiCrMoV martensitic steel,[18] however, it is two to three times higher than for a martensitic advanced high strength-steel[17] and a dual phase steel.[19] It is emphasized that the surface condition during gas permeation differs significantly from the inside of a pipeline in operation, for example, presence of an oxide layer. However, pipelines are subjected to cyclic stresses caused by pressure fluctuations which can rupture an oxide layer and expose the bare steel surface. It is reported in the literature, that exposure to pressurized hydrogen gas reduces the fracture toughness and increases the fatigue crack growth rate of pipeline steels,[4–6] indicating that hydrogen uptake occurs locally. The linearity between C_{0R} and $f_{H_2}^{1/2}$ and S being comparable to reported values suggests that the Pd-coated surface can resemble the hydrogen uptake of a bare steel surface after breakage of an oxide layer, however, this should be investigated further. In Figure 2c, the C_{0R} obtained at CP simulated conditions is superimposed onto the linear regression line determined for Sieverts' law, which corresponds to a $f_{H_2}^{eq}$ of 12.4 bar. Based on Equation (5), $p_{H_2}^{eq}$ is 12.3 bar, which is significantly lower than the desired hydrogen pressure of 200 bar.

Two methods to increase the hydrogen uptake are the addition of a hydrogen recombination poison,[22,26] or to modify the cathodic charging parameters (i.e., apply a more negative potential or higher cathodic current density).[15,25] Based on the previous study,[16] a $p_{H_2}^{eq}$ of 196.4 bar was obtained at a current density of −50 mA cm^{-2}

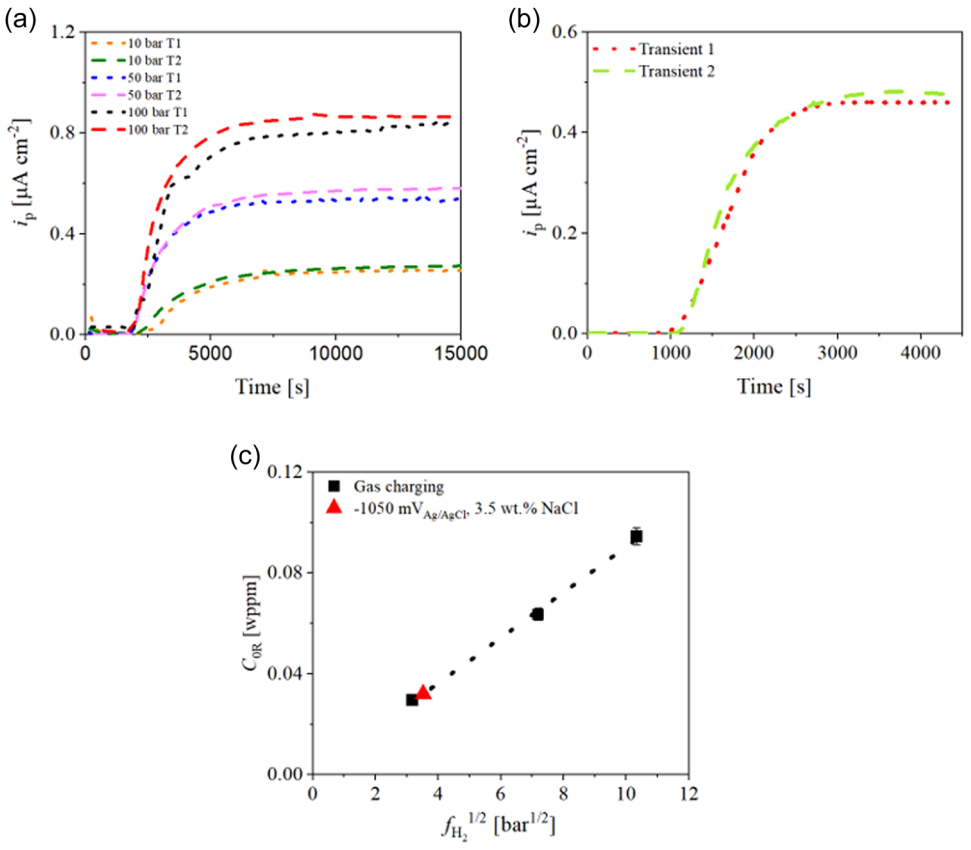

FIGURE 2 (a) Hydrogen permeation transients obtained at 10, 50, and 100 bar hydrogen gas charging pressures. (b) Hydrogen permeation transients were obtained at −1050 mV$_{Ag/AgCl}$ in a 3.5 wt% NaCl solution. (c) Subsurface hydrogen concentration, C_{0R}, versus the square root of hydrogen gas fugacity, $f_{H_2}^{1/2}$, with C_{0R} obtained at −1050 mV$_{Ag/AgCl}$ in a 3.5 wt% NaCl solution superimposed onto Sieverts' law regression line. [Color figure can be viewed at wileyonlinelibrary.com]

(corresponding to a potential of about −2600 $mV_{Ag/AgCl}$). However, it can be difficult to maintain stable surface conditions at such high cathodic current density. Unsteady surface conditions can be a result of excessive hydrogen bubble formation or changes in local pH, leading to fluctuations in hydrogen flux or detachment of inclusions.[26,27,40] In addition, the increasing influence of electrochemical recombination at higher cathodic current densities[41] can reduce the effect of applied current density or potential on the $p_{H_2}^{eq}$. Consequently, it was decided to use a hydrogen recombination poison as the first measure to increase the hydrogen absorption, before changing the applied cathodic potential.

Thiourea is a hydrogen recombination poison often used to enhance the hydrogen uptake.[21] Hydrogen permeation transients obtained at a cathodic potential of −1050 $mV_{Ag/AgCl}$ in a 3.5 wt% NaCl solution with 0–3 g L^{-1} thiourea, are shown in Figure 3a. An addition of 0.5 g L^{-1} thiourea increases i_p^{∞} by approximately 2.5 times compared to the pure 3.5 wt% NaCl solution. Further, the additions of 1.0 and 2.0 g L^{-1} thiourea about triples i_p^{∞}. The $p_{H_2}^{eq}$ values as a function of thiourea concentration are presented in Figure 3b. It can be observed that $p_{H_2}^{eq}$ increases initially with an increasing thiourea concentration until 2 g L^{-1}, where a decrease in $p_{H_2}^{eq}$ started. The reduced hydrogen uptake at high hydrogen recombination poison concentration could be attributed to the formation of deposits acting as an inhibiting layer to hydrogen uptake.[42] Because the addition of thiourea reached its limit contribution in $p_{H_2}^{eq}$ at 111.5 bar, it was necessary to apply more negative cathodic potential to obtain the desired $p_{H_2}^{eq}$ of 200 bar.

Hydrogen permeation transients obtained with different applied cathodic potentials in a 3.5 wt% NaCl solution with 2 g L^{-1} thiourea concentration are presented in Figure 4a. The i_p^{∞} increases when more negative cathodic potentials are applied. Compared with that obtained at −1050 $mV_{Ag/AgCl}$, i_p^{∞} increases by 1.17 times at −1125 $mV_{Ag/AgCl}$, 1.35 times at −1200 $mV_{Ag/AgCl}$, and 1.68 times at −1275 $mV_{Ag/AgCl}$. Table 2 lists the determined C_{0R}, $f_{H_2}^{eq}$, and $p_{H_2}^{eq}$. At −1200 and −1275 $mV_{Ag/AgCl}$ the $p_{H_2}^{eq}$ obtained are 191.4 and 237.4 bar, respectively. Hence, the desired $p_{H_2}^{eq}$ of 200 bar should be obtained between these two potentials. To determine the potential at which a 200 bar $p_{H_2}^{eq}$ would be obtained, $f_{H_2}^{eq}$ is plotted on a logarithmic scale as a function of applied potential, as illustrated in Figure 4b. By using Equation (5), it is calculated that a 200 bar p_{H_2} corresponds to a f_{H_2} of 227.2 bar. The relationship between $f_{H_2}^{eq}$ and applied potential from Figure 4b was solved for 227.2 bar, and the determined corresponding potential was approximately −1225 $mV_{Ag/AgCl}$. Following the above deduction, a permeation transient was performed at a potential of −1225 $mV_{Ag/AgCl}$ in 3.5 wt% NaCl solution with 2 g L^{-1} thiourea concentration, and the results are included in Table 2. The corresponding C_{0R} is 0.137 wppm and the $p_{H_2}^{eq}$ is 201.9 bar. Thus, electrochemical charging at a potential −1225 $mV_{Ag/AgCl}$ in 3.5 wt% NaCl solution with 2 g L^{-1} thiourea concentration can represent approximately the same C_{0R} as a $p_{H_2}^{eq}$ of 200 bar. The determined equivalence in terms of hydrogen uptake was obtained with a Pd coating during gas permeation. However, in real service conditions, the equivalence can be affected by relevant environmental parameters (e.g., the presence of surface oxides, temperature, and local stress conditions), which should be carefully considered in the design of HE susceptibility investigations. In addition, the transferability of the determined equivalent hydrogen pressure to mechanical testing needs to be validated.

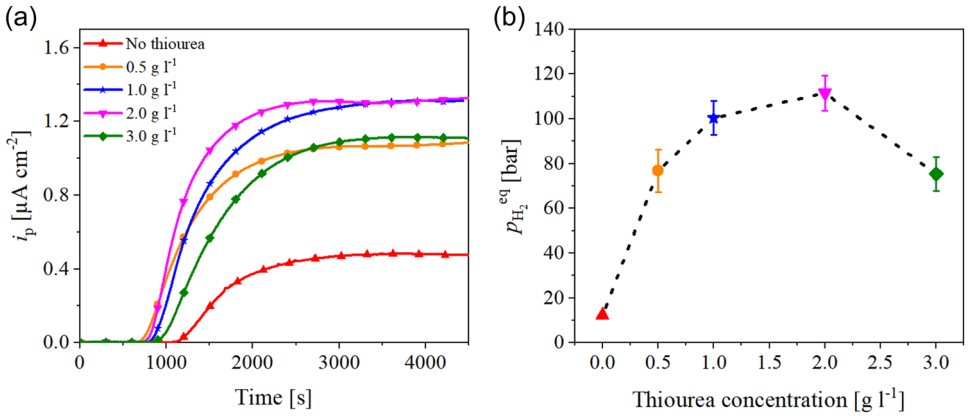

FIGURE 3 (a) Hydrogen permeation transients obtained at −1050 $mV_{Ag/AgCl}$ in a 3.5 wt% NaCl solution with different thiourea concentrations. (b) Equivalent hydrogen pressure, $p_{H_2}^{eq}$, versus the thiourea concentration. [Color figure can be viewed at wileyonlinelibrary.com]

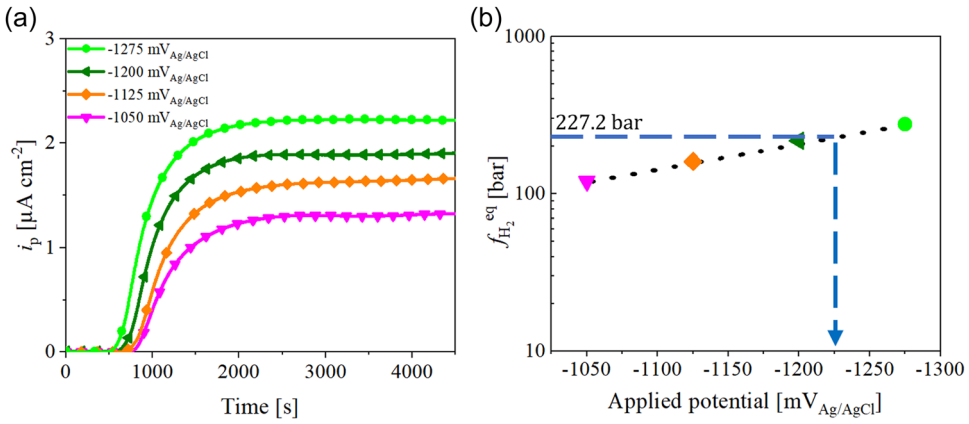

FIGURE 4 (a) Hydrogen permeation transients performed at different cathodic potentials in a 3.5 wt% NaCl solution with 2 g L^{-1} thiourea. (b) Equivalent hydrogen fugacity, $f_{H_2}^{eq}$, versus the applied potential. [Color figure can be viewed at wileyonlinelibrary.com]

TABLE 2 C_{0R}, $f_{H_2}^{eq}$, and $p_{H_2}^{eq}$ obtained by charging at different cathodic potentials in a 3.5 wt% NaCl solution with 2 g L^{-1} thiourea.

Potential ($mV_{Ag/AgCl}$)	C_{0R} (wppm)	$f_{H_2}^{eq}$ (bar)	$p_{H_2}^{eq}$ (bar)
−1050	0.099 ± 0.004	119.8 ± 9.0	111.5 ± 7.8
−1125	0.115 ± 0.002	160.0 ± 4.3	145.7 ± 3.6
−1200	0.133 ± 0.001	216.3 ± 2.7	191.4 ± 2.2
−1225	0.137 ± 0.001	229.7 ± 1.5	201.9 ± 1.2
−1275	0.151 ± 0.002	276.3 ± 7.2	237.4 ± 5.4

4 | CONCLUSIONS

This study established an equivalence between electrochemical and gaseous hydrogen charging by the addition of a hydrogen recombination poison in combination with different charging potentials. The results show that the subsurface hydrogen concentration was proportional to the square root of the hydrogen fugacity, in agreement with Sieverts' law, which formed the basis for determining the equivalent hydrogen pressure. Electrochemical charging at the condition simulating cathodic protection at −1050 $mV_{Ag/AgCl}$ was equivalent to a hydrogen pressure of 12.3 bar at room temperature. Higher equivalent pressures were achieved by adding thiourea to the 3.5 wt% NaCl solution, and by applying more negative cathodic potentials. The equivalent pressure as a function of thiourea concentration went through a maximum at 2 g L^{-1}. The desired equivalent pressure of about 200 bar, which is a potential hydrogen pressure during hydrogen gas transportation using pipeline steel, was obtained in a 3.5 wt% NaCl solution with 2 g L^{-1} thiourea and an applied potential of −1225 $mV_{Ag/AgCl}$ at room temperature. The equivalent hydrogen pressure was deduced using a Pd coating during gas permeation, and further evaluation must be conducted to elucidate the effect of surface conditions and transferability to mechanical testing.

ACKNOWLEDGMENTS

The authors acknowledge the financial support by the Research Council of Norway and the industry company partners through the HyLINE project (294739).

CONFLICT OF INTEREST STATEMENT

The authors declare no conflict of interest.

DATA AVAILABILITY STATEMENT

The data that support the findings of this study are available from the corresponding author upon reasonable request.

ORCID

Erik Koren http://orcid.org/0009-0009-3790-9756
Roy Johnsen http://orcid.org/0000-0002-5449-7396

REFERENCES

[1] Z. Abdin, A. Zafaranloo, A. Rafiee, W. Mérida, W. Lipiński, K. R. Khalilpour, *Renew. Sustain. Energy Rev.* **2020**, *120*, 109620.
[2] N. E. Nanninga, Y. S. Levy, E. S. Drexler, R. T. Condon, A. E. Stevenson, A. J. Slifka, *Corros. Sci.* **2012**, *59*, 1.
[3] J. Yamabe, T. Awane, S. Matsuoka, *Int. J. Hydrogen Energy* **2015**, *40*, 11075.
[4] L. Briottet, I. Moro, P. Lemoine, *Int. J. Hydrogen Energy* **2012**, *37*, 17616.
[5] T. An, H. Peng, P. Bai, S. Zheng, X. Wen, L. Zhang, *Int. J. Hydrogen Energy* **2017**, *42*, 15669.
[6] E. S. Drexler, A. J. Slifka, R. L. Amaro, N. Barbosa, D. S. Lauria, L. E. Hayden, D. G. Stalheim, *Fatigue Fracture Eng. Mater. Struct.* **2014**, *37*, 517.

[7] S. Cerniauskas, A. J. Chavez Junco, T. Grube, M. Robinius, D. Stolten, *Int. J. Hydrogen Energy* **2020**, *45*, 12095C12107.
[8] L. Briottet, R. Batisse, G. de Dinechin, P. Langlois, L. Thiers, *Int. J. Hydrogen Energy* **2012**, *37*, 9423.
[9] S. Lynch, *Corros. Rev.* **2012**, *30*, 105.
[10] G. B. Rawls, T. Adams, N. L. Newhouse in *Gaseous hydrogen embrittlement of materials in energy technologies*, Vol. 1 (Eds: R. P. Gangloff, B. P. Somerday), Woodhead Publishing Series in Metals and Surface Engineering, London **2012**, p. 3.
[11] A. Turnbull, in *Gaseous hydrogen embrittlement of materials in energy technologies*, Vol. 1 (Eds: R. P. Gangloff, B. P. Somerday), Woodhead Publishing Series in Metals and Surface Engineering, London **2012**, p. 89.
[12] P. Zhang, M. Laleh, A. E. Hughes, R. K. W. Marceau, T. Hilditch, M. Y. Tan, *Int. J. Hydrogen Energy* **2023**, *48*, 16501.
[13] A. J. Kumnick, H. H. Johnson, *Metall. Trans. A* **1975**, *6*, 1087.
[14] A. Atrens, D. Mezzanotte, N. F. Fiore, M. A. Genshaw, *Corros. Sci.* **1980**, *20*, 673.
[15] Q. Liu, A. D. Atrens, Z. Shi, K. Verbeken, A. Atrens, *Corros. Sci.* **2014**, *87*, 239.
[16] E. Koren, C. M. H. Hagen, D. Wang, X. Lu, R. Johnsen, J. Yamabe, *Corros. Sci.* **2023**, *215*, 111025.
[17] J. Venezuela, E. Gray, Q. Liu, Q. Zhou, C. Tapia-Bastidas, M. Zhang, A. Atrens, *Corros. Sci.* **2017**, *127*, 45.
[18] J. Venezuela, C. Tapia-Bastidas, Q. Zhou, T. Depover, K. Verbeken, E. Gray, Q. Liu, Q. Liu, M. Zhang, A. Atrens, *Corros. Sci.* **2018**, *132*, 90.
[19] Q. Liu, E. Gray, J. Venezuela, Q. Zhou, C. Tapia-Bastidas, M. Zhang, A. Atrens, *Adv. Eng. Mater.* **2018**, *20*, 1700469.
[20] J. L. Crolet, G. Maisonneuve, *NACE Corrosion 2000*, NACE International, Houston **2000**.
[21] T. Depover, D. Pérez Escobar, E. Wallaert, Z. Zermout, K. Verbeken, *Int. J. Hydrogen Energy* **2014**, *39*, 4647.
[22] E. Akiyama, S. Li, *Corros. Rev.* **2016**, *34*, 103.
[23] E. Protopopoff, P. Marcus, in *Corrosion mechanisms in theory and practice* (Ed: P. Marcus), CRC Press Taylor and Francis Group, Boca Raton **2011**, p. 105.
[24] B. J. Berkowitz, J. J. Burton, C. R. Helms, R. S. Polizzotti, *Scripta Metall.* **1976**, *10*, 871.
[25] L. Zhang, W. Cao, K. Lu, Z. Wang, Y. Xing, Y. Du, M. Lu, *Int. J. Hydrogen Energy* **2017**, *42*, 3389.
[26] Y. J. Jeong, S. J. Kim, *Int. J. Hydrogen Energy* **2021**, *46*, 7615.
[27] J. Flis, *Electrochim. Acta* **1999**, *44*, 3989.
[28] H. Husby, M. Iannuzzi, R. Johnsen, M. Kappes, A. Barnoush, *Int. J. Hydrogen Energy* **2018**, *43*, 3845.
[29] P. Bruzzoni, *Int. J. Hydrogen Energy* **2000**, *25*, 61.
[30] P. Castaño Rivera, V. P. Ramunni, P. Bruzzoni, *Corros. Sci.* **2012**, *54*, 106.
[31] P. Manolatos, M. Jerome, J. Galland, *Electrochim. Acta* **1995**, *40*, 867.
[32] M. A. V. Devanathan, Z. Stachurski, *Proc. R. Soc. Lond. Ser. A. Math. Phys. Sci.* **1962**, *270*, 90.
[33] T. Zakroczymski, *Electrochim. Acta* **2006**, *51*, 2261.
[34] ISO 17081:2014, *Method of measurement of hydrogen permeation and determination of hydrogen uptake and transport in metals by an electrochemical technique*, International Organization for Standardization **2014**.
[35] C. K. Gupta, *Chemical Metallurgy: Principles and Practice*, Wiley-VCH, Weinheim **2003**.
[36] A. Turnbull, *Int. J. Hydrogen Energy* **2015**, *40*, 16961.
[37] C. San Marchi, B. Somerday, S. Robinson, *Int. J. Hydrogen Energy* **2007**, *32*, 100.
[38] K. Kiuchi, R. B. McLellan, *Acta Metall.* **1983**, *31*, 961.
[39] A. Turnbull, *Mater. Sci. Forum* **1995**, *192-194*, 63.
[40] S. M. Charca, O. N. C. Uwakweh, V. S. Agarwala, *Metall. Mater. Trans. A* **2007**, *38*, 2389.
[41] J. O. Bockris, J. McBreen, L. Nanis, *J. Electrochem. Soc.* **1965**, *112*, 1025.
[42] E. Lunarska, Z. Szklarska-Smialowska, M. Smialowski, *Mater. Corros.* **1975**, *26*, 324.

How to cite this article: E. Koren, C. M. H. Hagen, D. Wang, X. Lu, R. Johnsen, *Mater. Corros.* **2024**, *75*, 315–321. https://doi.org/10.1002/maco.202313931